Biomacromolecules

ARTICLE

pubs.acs.org/Biomac

Bioinspired Imprinted PHEMA-Hydrogels for Ocular Delivery of Carbonic Anhydrase Inhibitor Drugs

Andreza Ribeiro,[†,‡,§] Francisco Veiga,[†,‡] Delfim Santos,[‡,∥] Juan J. Torres-Labandeira,[§] Angel Concheiro,[§] and Carmen Alvarez-Lorenzo*[,§]

[†]Department of Pharmaceutical Technology and [‡]Centre for Pharmaceutical Studies, Faculty of Pharmacy, University of Coimbra, 3000-548-Coimbra, Portugal

[§]Departamento de Farmacia y Tecnología Farmacéutica, Facultad de Farmacia, Universidad de Santiago de Compostela, 15782-Santiago de Compostela, Spain

[∥]Department of Pharmaceutical Technology, Faculty of Pharmacy, University of Porto, 4050-047-Porto, Portugal

ABSTRACT: Hydrogels with high affinity for carbonic anhydrase (CA) inhibitor drugs have been designed trying to mimic the active site of the physiological metallo-enzyme receptor. Using hydroxyethyl methacrylate (HEMA) as the backbone component, zinc methacrylate, 1- or 4-vinylimidazole (1VI or 4VI), and *N*-hydroxyethyl acrylamide (HEAA) were combined at different ratios to reproduce in the hydrogels the cone-shaped cavity of the CA, which contains a Zn^{2+} ion coordinated to three histidine residues. 4VI resembles histidine functionality better than 1VI, and, consequently, pHEMA-$ZnMA_2$ hydrogels bearing 4VI moieties were those with the greatest ability to host acetazolamide or ethoxzolamide (2 to 3 times greater network/water partition coefficient) and to sustain the release of these antiglaucoma drugs (50% lower release rate estimated by fitting to the square root kinetics). The use of acetazolamide as template during polymerization did not enhance the affinity of the network for the drugs. In addition to the remarkable improvement in the performance as controlled release systems, the biomimetic hydrogels were highly cytocompatible and possessed adequate oxygen permeability to be used as medicated soft contact lenses or inserts. The results obtained highlight the benefits of mimicking the structure of the physiological receptors for the design of advanced drug delivery systems.

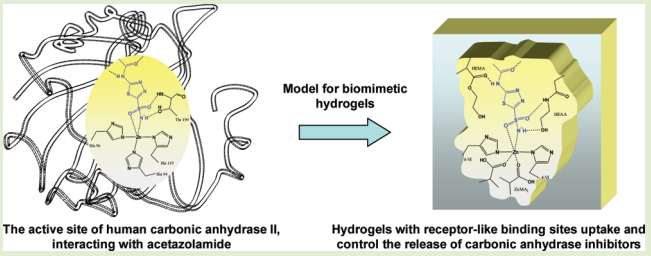

INTRODUCTION

Glaucoma is a progressive disease that causes optic nerve head damage. Currently, its prevalence is a high as 1% in people aged 40−49 years and up to 8% above 80 years old and is one of the most common causes of blindness.[1,2] The elevation of the intraocular pressure (IOP) is the main risk factor for glaucoma because of compression of the optic nerve fibers against the lamina cribrosa or ischemia associated to the disturbance of the blood supply to the nerve. In open-angle glaucoma, there is impaired flow of aqueous humor through the trabecular meshwork-Schlemm's canal venous system.[3] The first choice of glaucoma treatment is the medical therapy with the goal of lowering the IOP to a level at which the damage of the optic nerve ceases to progress. Adrenergic drugs, mainly β-antagonists (such as timolol) alone or combined with β-agonists (epinephrine) or α-agonists (brimonidine), cholinergic drugs (pilocarpine), carbonic anhydrase inhibitors (CAIs; e.g., acetazolamide, ethoxzolamide), cannabinoids, and prostaglandins have been shown to be useful to decrease the IOP.[4] Systemic delivery, mainly through the oral route, is, however, accompanied by relevant side effects, which are in most cases associated with the doses required to achieve therapeutic concentration at the ocular site. Ophthalmic formulations, such as eye drops, are not exempt of collateral effects either, because <5% of the instilled dose is absorbed intraocularly. The rest pass through the conjuntiva or are removed from the eye surface by the defense mechanism that partially leads to nasolacrimal drainage; both routes may result in systemic absorption.[5] An ideal ocular drug delivery system should be able to increase ocular bioavailability, to prolong the duration of drug action, and to avoid large fluctuations in ocular drug concentration and ocular and systemic side effects.[6] In this context, soft contact lenses (SCLs) are gaining an increasing attention as combination products able to correct refractive deficiencies and to perform as sustained delivery systems.[7−11]

The feasibility of using drug-loaded SCLs depends on whether the drug and the hydrogel material can be matched so that the lens uptakes a sufficient quantity of drug and releases it in a controlled fashion. Most commercially available SCLs show a deficient performance because they release ophthalmic drugs too rapidly.[12,13] To overcome this drawback, the following approaches are being explored: (i) chemically reversible immobilization of drugs through labile bonds;[7,14] (ii) incorporation of drug-loaded colloidal systems into the lens;[15−17] (iii) copolymerization with functional monomers

Received: November 9, 2010
Published: February 11, 2011

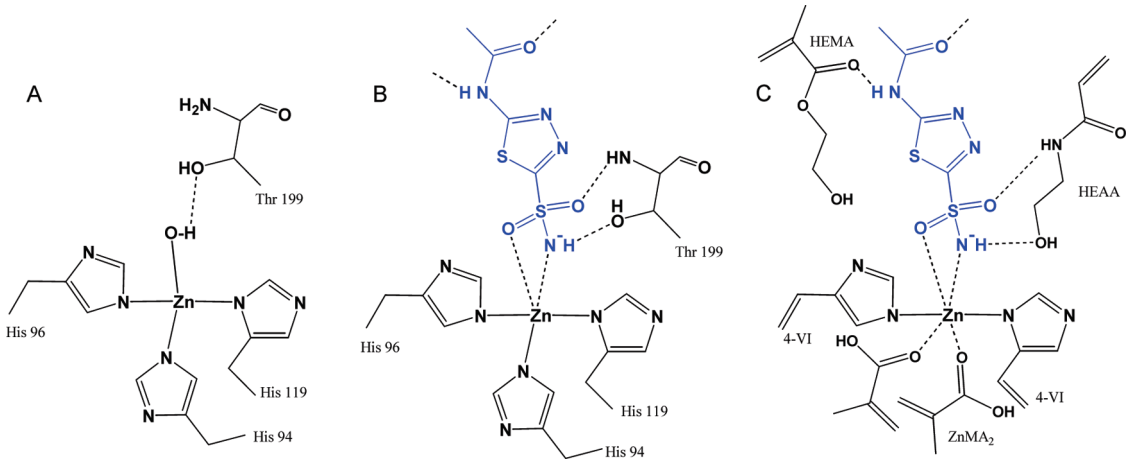

Figure 1. Schematic draw of the active site of human carbonic anhydrase II free (A) and after binding acetazolamide (B) as described by Lindskog,[37] and of the mimicking binding pockets expected to be created in the biomimetic hydrogels (C).

able to interact directly with the drug;[18−20] and (iv) molecular imprinting.[21−25] This last technique aims to organize the components of the hydrogel network in such a way that high affinity binding sites for the drug are created. To do that, the drug is added before polymerization, and the monomers should arrange as a function of their ability to interact with the drug molecules. After polymerization, the drug molecules that have acted as templates are removed, and the polymer network may exhibit "tailored-active sites" or "imprinted pockets" with the size and the most suitable chemical groups to interact again with the drug.[26,27] A distinguishing key feature of SCLs is their relatively low cross-linking density compared with common imprinted networks, which can compromise the physical stability of the imprinted cavities due to swelling after synthesis. Only high affinity cavities can memorize the structural features of the drug and undergo an "induced fit" in the presence of the drug recovering the same conformation as upon polymerization.[22,28] In such a way, loosely cross-linked imprinted hydrogels try to mimic the recognition capacity of certain biomacromolecules (e.g., receptors, enzymes, antibodies). Natural evolution has determined the unique details of protein's native state, such as its shape and charge distribution, that enable it to recognize and interact with specific molecules.[29] On the basis of biomimetic principles, SCLs endowed with such high affinity imprinted pockets are expected to be able to load the drug and, subsequently, to sustain the release. Ultrathin SCLs synthesized applying the molecular imprinting technology have already demonstrated greater uptake of timolol and better in vivo control of drug release to the lacrimal fluid than conventional SCLs and eyedrops, using similar or even lower doses.[30] The selection of the functional monomers responsible for the interaction with the drug can be carried out applying analytical techniques[25] and computational modeling[31,32] for the screening of monomers libraries or according to a configurational biomimesis based on the chemical functionality of the natural receptors.[27,33] Byrne et al. have recently shown that the selection of functional monomers possessing chemical groups similar to those present in the histamine H1-receptor or in the CD44 protein endows the hydrogels with high affinity for the antihistamic drug ketotifen fumarate[23,34] or for hyaluronic acid,[35] respectively. Imprinted hydrogels exhibited higher loading and delayed release compared with the nonimprinted ones, and it was demonstrated that each functional monomer relating to the biological binding played a role in the delayed release.[23,34,35]

The aim of this work was to design SCLs with high affinity for CAIs, such as acetazolamide and ethoxzolamide (ETOX), applying biomimetic principles and the molecular imprinting technology. The idea is to create binding pockets in the network structure that resemble the active site of CA to mime the noncovalent interactions responsible for the docking of the CAIs in the physiological receptor. Carbonic anhydrases are metalloenzymes that catalyze the conversion of carbon dioxide to bicarbonate ion and protons.[36] Although there are different isoforms, the active site of most of them consists of a cone-shaped cavity that contains a Zn^{2+} ion coordinated to three histidine residues in a tetrahedral geometry with a solvent molecule as the fourth ligand[37] (Figure 1A). There are two main classes of CAIs: (i) the metal-complexing anions and (ii) the sulfonamides and their bioisosteres, which bind to the Zn^{2+} ion of the enzyme either by substituting the nonprotein zinc ligand to generate a tetrahedral adduct or by addition to the metal coordination sphere, generating trigonal-bipyramidal species.[38] The −NH function of the ionized sulfonamide group replaces the water molecule bound to zinc and the hydrogen bonds to the −OH group of threonine 99. One oxygen atom of the sulfonamide interacts with the −NH group of treonine 199, whereas another oxygen points toward the zinc ion (Figure 1B). Other chemical groups of the CAIs establish van der Waals interactions or hydrogen bonds with neighbor amino acids.[37] Therefore, monomers bearing chemical groups similar to those of the amino acids involved in the active binding site were chosen to prepare biomimetic hydrogels: the zinc ions were introduced as methacrylate salt ($ZnMA_2$); the hydroxyl and amino groups can be supplied by 2-hydroxyethyl methacrylate (HEMA) and *N*-hydroxyethyl acrylamide (HEAA); and 4-vinylimidazole (4VI) resembles histidine (Figure 1C). 4VI is not commercially available, and thus the first step was to synthesize it. For comparative purpose, 1-vinylimidazole (1VI) was also included in the study as an alternative for 4VI in the mimicking of histidine (Figure 2). Then, a set of hydrogels with fix content in $ZnMA_2$ and various comonomer combinations was prepared and characterized regarding their ability to load and to sustain the release of acetazolamide and ETOX. Cytocompatibility, degree of swelling, and other relevant features from the point of view of the use of the hydrogels as components of SCLs were also evaluated.

EXPERIMENTAL SECTION

Materials. Acetazolamide (ACT), ETOX, HEMA, ethyleneglycol dimethacrylate (EGDMA), zinc methacrylate ($ZnMA_2$), 1VI, urocanic acid, and HEAA were from Sigma-Aldrich Chemicals (Madrid, Spain) (Figure 2). Azobisisobutyronitrile (AIBN) was from Acros Organic (Geel, Belgium). Zincon monosodium salt (2-carboxy-2′-hydroxy-5′-sulfoformazylbenzene) and zinc nitrate hexahydrate were from Sigma-Aldrich (St. Louis MO). Purified water was obtained by reverse osmosis (Milli-Q, Millipore Ibérica SA, Madrid, Spain). Other reagents were analytical grade.

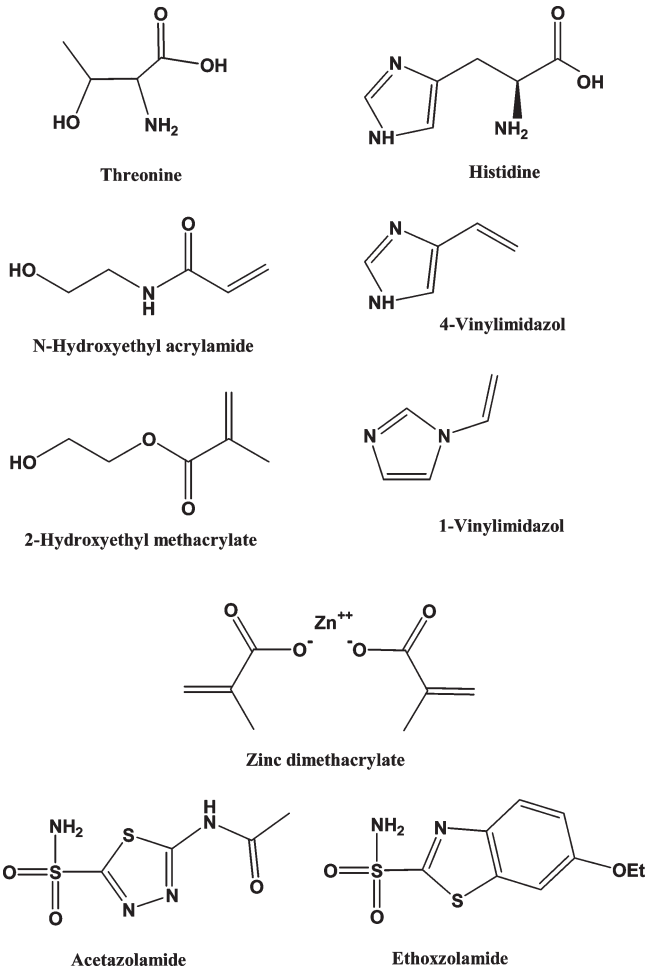

Figure 2. Amino acids that form part of the active site of carbonic anhydrase, monomers used to synthesize the hydrogels, and CAI drugs tested.

Synthesis of 4(5)-Vinylimidazole (4VI). 4VI was obtained via thermal decarboxylation from urocanic acid according to the literature.[39] In brief, anhydrous urocanic acid (2 g, 0.0145 mol) was placed in a short-necked distilling apparatus. Then, the temperature was slowly increased to 205 °C under pressure of 18 Torr. The distilled material was trapped using a glass sink (coldfinger) cooling system. 4VI was obtained as a crystallized white product in the cold receiver (yield = 12%). Then, it was stored in the fridge at 4 °C. The obtaining of 4VI was confirmed by FTIR-ATR spectroscopy (400−4000 cm^{-1}, Varian-670-FTIR spectrometer equipped with a GladiATR, Madison, WI) and ^1H NMR analysis (Varian Mercury 300 MHz + robot spectrophotometer, Madison, WI). The peaks of 4VI in $CDCl_3$ were assigned as follows: δ 5.10 (d, J = 12.15 Hz, 1H), 5.65 (d, J = 17.64 Hz, 1 H), 6.60 (m, 1H), 7.02 (s, 1H), 7.61 (s, 1H), 10.32 (br s, 1H).[40]

Synthesis of pHEMA Hydrogels. Various sets of monomer mixtures were prepared with the composition shown in Table 1. ACT was added to some mixtures at a concentration of 7.8×10^{-4} M to attain a molar ratio of 1:1:3 for drug/Zn^{2+}/VI. The monomer solutions were injected into molds constituted by two glass plates pretreated with dimethyldichlorosilane and separated by a silicone frame of 0.9 mm thickness.[41] The molds were placed in an oven at 50 °C for 12 h and then heated to 70 °C for 24 h more. The hydrogels were removed from the molds and immersed in boiling water (600 mL) for 15 min to remove nonreacted components and to facilitate the cutting of the hydrogels as 10 mm discs. The discs were washed in ultra pure water for 24 h, in NaCl 0.9% solution for 24 h and then immersed in water for 15 days (400 mL). We monitored the removal of unreacted monomers by measuring the absorbance in the 190−800 nm range of the washing solutions. Finally, the discs were dried and stored.

Determination of Zinc Content. We prepared a stock solution of Zincon (1.6 mM) by dissolving 7.4 mg in 250 μL of 1 M NaOH prior to dilution to 10 mL with water. The solution was kept in the fridge and used in a few days. Zn^{2+} stock solution (27 mM) was prepared by dissolving zinc nitrate hexahydrate in 50 mL of 0.1 M nitric acid. The calibration curve was constructed by adding 25 μL of diluted stock solution (0.31 to 1.25 mM) to 950 μL of USP borate buffer pH 9.0 and 25 μL of the Zincon stock solution.[42] The blank was prepared analogously except for the substitution of the metal sample solution with 0.1 M nitric acid. Absorption spectra were recorded from 400 to 750 nm after 5 min of sample incubation at room temperature. The absorbances were measured at 620 nm. The intensity of the blue color was proportional to the zinc concentration.[42] To quantify the amount of zinc present in the hydrogels, we transferred dried discs to test tubes containing 2 mL of 1.0 M nitric acid kept at 70 °C for ~48 h. Aliquots (100 μL) of the final solution were diluted with 330 μL of 1.0 M nitric

Table 1. Composition of the Monomer Mixtures Used to Synthesize the Hydrogels

formulation	HEMA (mL)	$ZnMA_2$ (g)	HEAA (g)	1VI (mL)	4VI (g)	EGDMA (mL)	AIBN (g)	ACT (g)
0	8					0.12	0.0135	
A	8	0.185				0.12	0.0135	
B	8	0.185				0.12	0.0135	0.173
C	8	0.185		0.22		0.12	0.0135	
D	8	0.185		0.22		0.12	0.0135	0.173
E	8	0.185			0.22	0.12	0.0135	
F	8	0.185			0.22	0.12	0.0135	0.173
G	8	0.185	0.14			0.12	0.0135	
H	8	0.185	0.14			0.12	0.0135	0.173
I	8	0.185	0.14		0.22	0.12	0.0135	
J	8	0.185	0.14		0.22	0.12	0.0135	0.173

acid and then mixed with 70 μL of NaOH 5 M to adjust the pH to 4 to 5. Then, 25 μL of the resulting solution was added to 950 μL of USP borate buffer pH 9.0 and 25 μL of the Zincon stock solution and incubated at room temperature for 5 min. The absorbance was recorded at 620 nm, and the amount of zinc in the sample was estimated from the calibration curve. All experiments were carried out in triplicate.

Physical and Structural Characterization of pHEMA Hydrogels. FTIR-ATR (attenuated total reflection) spectra were recorded over the range 400−4000 cm^{-1}, in a Varian-670-FTIR spectrometer equipped with a GladiATR (Madison, WI) with diamond crystal. DSC scans of dried hydrogels (5−10 mg) were recorded by heating from 25 to 150 °C, cooling to −10 °C, and then heating again until 300 °C, always at the rate of 10 °C/min, in a DSC Q100 (TA Instruments, New Castle, DE) with a refrigerated cooling accessory. Nitrogen was used as purge gas at a flow rate of 50 mL/min. The calorimeter was calibrated for cell constant and temperature using indium standard (melting point 156.61 °C, enthalpy of fusion 28.71 J/g) and for heat capacity using sapphire standards. All experiments were performed in duplicate. Degree of swelling in water was calculated, in duplicate, as follows

$$Q(\%) = \frac{(W_t - W_0)}{W_0} \cdot 100 \quad (1)$$

where W_0 and W_t represent the weights of a hydrogel disc at the dry state and after being immersed in water for a time t. Light transmittance of fully swollen hydrogels was recorded in triplicate at 600 nm (UV−vis spectrophotometer, Agilent 8453, Boeblingen, Germany) by mounting a continuous piece of hydrogel on the inside face of a quartz cell. Oxygen permeability (Dk) and transmissibility of hydrogels previously swollen in a 0.9% NaCl solution were measured in triplicate at room temperature using a Createch permeometer (model 210T, Rehder Development Company, Castro Valley) fitted with a flat polarographic cell and in a chamber at 100% of relative humidity.

Cytocompatibility Studies. Dried discs were immersed in phosphate buffer (pH 7.4) and autoclaved (121 °C, 20 min). Cytocompatibility tests were carried out in triplicate using the Balb/3T3 Clone A31 cell line (ATCC, LGC Standards S.L.U., Barcelona, Spain) according to the direct contact test of the ISO 10993-5:1999 standard. The discs were added in 24-well plates containing 200 000 cells per well in 2 mL of Dulbecco's modified Eagle's medium F12HAM supplemented with 10% fetal bovine serum and 13 μg/mL gentamicin. The plates were incubated at 37 °C, 5% of CO_2, and 90% of humidity. After 24 h, aliquots (100 μL) of medium were taken in 96-well microplates and mixed with reaction mixture solution (100 μL, Cytotoxicity Detection Kit, LDH, Roche). The plates were incubated at 20 °C for 30 min (protected from light). A stop solution (50 μL) was added to the wells and the absorbance was measured at 490 nm (BIORAD model 680 Microplate reader). Blank (culture medium), negative (cells in culture medium), and positive (cells in medium with lysis factor) controls were prepared too, and the was absorbance measured. The cytocompatibility was quantified as follows

$$\text{cytocompatibility } (\%) = \frac{Abs_{\text{exp}} - Abs_{\text{negativecontrol}}}{Abs_{\text{positivecontrol}} - Abs_{\text{negativecontrol}}} \quad (2)$$

ACT Loading and Release. Dried hydrogel discs (six replicates) were placed in 5 mL of ACT 0.2 g/L aqueous solution and kept at room temperature protected from the light for 48 h. The amount of ACT loaded was calculated as the difference between the initial amount of drug in the solution and the amount remaining after loading determined by UV spectrophotometry at 264 nm (Agilent 8453, Germany). Drug-loaded discs were rinsed with water, their surface was carefully wiped, and the discs were immediately immersed in 5 mL of NaCl 0.9% solution at room temperature. The amount of drug released was measured spectrophotometrically in samples periodically taken and again placed in the same vessel so that the liquid volume was kept constant. The network/water partition coefficient, $K_{N/W}$, which is an index of the affinity of the drug for the network, was estimated from the total amount loaded per gram of gel[43]

$$\text{loading}_{(\text{total})} = \left[\frac{(V_s + K_{N/W}V_p)}{W_p}\right] \cdot C_0 \quad (3)$$

where V_s is the volume of water sorbed by the hydrogel, W_p is the dried hydrogel weight, C_0 is the concentration of the drug in loading solution, and V_p is the volume of dried polymer.

Release profiles up to 60% released were fitted to the square-root kinetics as follows[44]

$$\frac{M_t}{M_\infty} = K_H \cdot t^{0.5} \quad (4)$$

where M_t represents the amount of drug released at time t and M_∞ is the total amount loaded. Each release profile was fitted to the Higuchi equation; then, the mean and the standard deviation were calculated from the values obtained for six replicates.

ETOX loading and Release. Dried hydrogels discs (six replicates) were placed in 5 mL of ETOX suspension (0.23 g/L) and kept for 48 h at room temperature. The ETOX-loaded discs were rinsed with water; their surfaces were carefully wiped, and the discs were immediately immersed in 5 mL of NaCl 0.9% at room temperature. The amount of drug released was measured spectrophotometrically at 303 nm in samples periodically taken up and placed again in the same vessel. After 360 h, the discs were removed from the medium, rinsed with ultrapure water, and placed in vials with 5 mL of ethanol/water (70:30) mixture for 48 h. The drug extracted from the hydrogels was quantified from the absorbance measured at 303 nm (Agilent 8453, Germany). The network/water partition coefficient, $K_{N/W}$, of ETOX was estimated from the total amount released to the aqueous medium plus that extracted in ethanol/water medium. ETOX solubility in water (21.38 mg/L) was used as C_0 in eq 3 because in the suspension, this concentration should remain constant. The release rate constants were estimated using eq 4.

RESULTS AND DISCUSSION

Hydrogels Synthesis and Structural Characterization. The hydrogels were prepared using HEMA as main component because of the recognized biocompatibility of pHEMA and its common use as integrant of SCLs.[45] Several monomers were copolymerized with HEMA to mimic the active site of CA (Table 1); the biomimetic level is foreseeable to increase from A to J formulations. A control pHEMA hydrogel without functional comonomers (formulation 0) was used as a reference to quantify the role of the comonomers in the binding of the CAIs. Although 4VI resembles much better than 1VI the functional groups of histidine, both monomers were used to prepare the hydrogels with the purpose of elucidating the incidence of the imidazole structure on the affinity for the CAIs. 4VI was successfully synthesized from urocanic acid, and its structure was confirmed by ^{1}H NMR (Figure 3). Urocanic acid showed chemical shifts at 2.49 and 3.32 ppm (−OH) and 6.32 ppm (CH═), whereas 4VI showed two singlet peaks at 7.03 and 7.61 ppm for N−CH and N═CH protons (imidazole), respectively. The methylene (CH_2═) and methane (CH═) protons of 4VI appeared at 5.16, 5.67, and 6.63 ppm according to the literature.[46]

The hydrogels were intensively washed after synthesis to remove the template molecules. Both imprinted and nonimprinted hydrogels underwent the same cleaning procedure. Because in the natural receptor, zinc directly participates in the binding of the drug (Figure 1B), we first corroborated the presence of zinc ions in the networks. It is interesting to note that even after boiling and immersion in saline medium, zinc ions were still detected in A to J hydrogel formulations (Table 2). Nevertheless, remarkable differences among the hydrogels could be observed; the imidazole monomers were absolutely required to keep significant amounts of zinc in the network. The small amount of zinc ions remaining in the hydrogels without 4VI could be due to the fact that $ZnMA_2$ is not reacting during polymerization or that zinc ions are replaced by counterions in the absence of 4VI. Because all hydrogels have a similar monomeric composition (HEMA being the majority monomer) and 100% zinc complexation can only be achieved if methacrylate mers are effectively copolymerized in the network, it is perfectly plausible that $ZnMA_2$ is similarly incorporated to all hydrogels. Therefore, the decrease in zinc ions can be attributed to the long extraction process in the presence of saline medium. Removal of zinc ions by sodium ions is not complete because the affinity of the methacrylic acid mers for divalent ions is larger than that for monovalent ones.[47] In sum, the formation of a zinc/methacrylic acid/imidazol coordination complex notably enhances the stability of the zinc bonds to the network. This finding is in agreement with previous papers that reported that polymers containing 1VI or 4VI can bind metal ions, including zinc, with a remarkable affinity even in saline medium.[48] Additionally, we observed that hydrogels bearing 4VI retained twice the amount of zinc ions (71−90%) than those synthesized with 1VI (38−43%). This finding can be related to the fact that 4VI mimics better the coordination of zinc to the amine groups of histidine residues that occurs in the natural CA enzyme. Because the affinity of zinc ions for methacrylic acid groups is quite high[47] and those zinc ions can still coordinate with two imidazole groups,[48] it seems that a quite plausible structure of the binding pocket is that depicted in Figure 1C. Nevertheless, other configurations of the receptor, such as that with only one imidazole group, cannot be discarded. The proportion of functional monomers in the hydrogel is too low for being able to gain an insight into this point using common analytical techniques.

The hydrogels were slightly opalescent because of the presence of $ZnMA_2$, particularly those prepared with 4VI (Table 2). Nevertheless, it should be noticed that the thickness of the hydrogels is larger (three- to four-fold) than that of commercial SCLs. Therefore, transmittance of thinner hydrogels might make possible to use some formulations as components of SCLs. The lower transmittance of the hydrogels prepared with 4VI can be also related to their lower degree of swelling in aqueous medium (Figure 4). pHEMA-$ZnMA_2$ hydrogels prepared without 1VI or 4VI (formulations A, B, G, and H) attained swelling values of 70−76% (Table 2), which are in the typical range value of

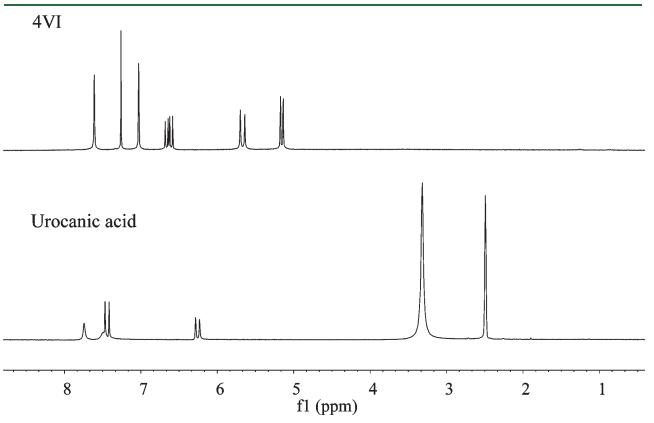

Figure 3. ^{1}H NMR spectra of urocanic acid in DMSO-d_6 and 4VI in $CDCl_3$.

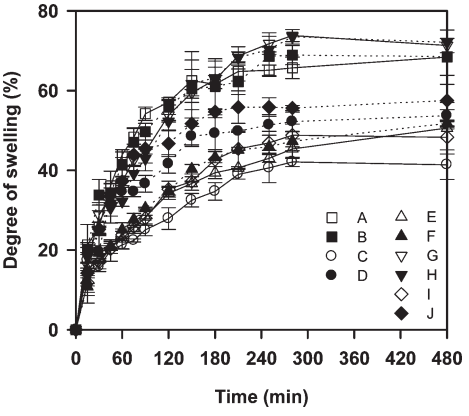

Figure 4. Swelling profiles of the pHEMA-$ZnMA_2$ hydrogels (codes as in Table 1) in water. Continuous and dotted lines correspond to nonimprinted and ACT-imprinted networks.

Table 2. Percentage of Zinc Ions That Remain in the Hydrogels after the Cleaning Step, And Physical Properties of the Networks. Mean Values and, In Parentheses, Standard Deviations

formulation	remaining Zn (%)	transmittance at 600 nm (%)	T_g (°C)	degree of swelling (%)	*Dk* (barrer)
0		85	110	66.0 (3.2)	12.4 (1.1)
A	22.6 (7.1)	76	109	73.0 (0.8)	12.6 (1.5)
B	11.3 (4.8)	70	115	70.6 (1.5)	17.7 (7.6)
C	38.7 (6.6)	68	126	42.8 (5.1)	9.2 (0.4)
D	43.7 (7.4)	64	132	55.5 (0.1)	12.8 (2.3)
E	73.6 (4.5)	29	125	52.7 (0.6)	14.8 (0.3)
F	71.9 (1.1)	29	125	53.4 (1.1)	13.4 (0.4)
G	10.0 (1.9)	73	110	77.5 (1.7)	18.0 (3.3)
H	13.9 (1.5)	77	109	75.2 (4.3)	24.8 (0.2)
I	76.9 (5.1)	22	116	55.5 (0.4)	17.2 (4.9)
J	90.8 (4.5)	30	123	61.0 (1.2)	15.6 (1.5)

dx.doi.org/10.1021/bm101562v |*Biomacromolecules* 2011, 12, 701–709

pHEMA hydrogels. Copolymerization with HEAA did not change the degree of swelling. In contrast, those hydrogels containing 1VI or 4VI exhibited a remarkably lower capability to sorb water (Table 2). The synthesis in the presence of ACT attenuated to a certain extent the decrease in the degree of swelling; the D, F, and J imprinted hydrogels swelled more in water than the corresponding C, E, and I nonimprinted networks.

Furthermore, 1VI and 4VI make the networks more rigid, as indicated by the increase in the glass-transition temperature, T_g, of the hydrogels prepared with these monomers (Table 2). The presence of $ZnMA_2$ did not alter the T_g of the pHEMA hydrogels, which is around 110 °C (Table 2). It has been reported that poly(1VI) has a T_g around 175 °C.[49] The DSC scans of the hydrogels containing 1VI or 4VI showed only one T_g, at an intermediate temperature between the T_g of pHEMA and that of poly(1VI), indicating that the monomers are miscible and confirming that the vinylimidazole monomers are efficiently copolymerized with the methacrylate ones.[39,46,49] Macromolecular interactions between the carbonyl group of ethyl methacrylate and the imidazol fragments have been previously shown by FTIR spectroscopy.[49] However, we could not observe relevant shifts in the carbonyl band at 1707 cm^{-1}, probably because of the relatively low proportion of 1VI and 4VI in the hydrogels compared with HEMA. The FTIR spectra mainly showed the characteristic bands of pHEMA (data not shown).

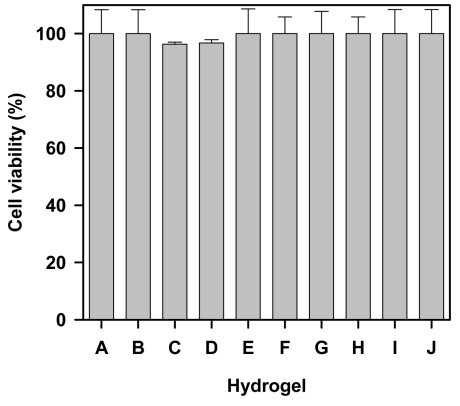

Figure 5. Cell viability for different pHEMA-$ZnMA_2$ hydrogels. Mean values and standard deviations (n = 3).

Oxygen Permeability and Cytocompatibility. Hydrogels intended as components of SCLs should have enough oxygen permeability for preventing corneal hypoxia and edema. As expected, the higher the degree of swelling, the greater the oxygen permeability of the hydrogels was (Table 2). This means that the hydrogels containing 1VI or 4VI are less gas-permeable than the other hydrogels. Nevertheless, the differences are not too large, and the values are in the range of those recorded for commercially available SCLs.[50,51]

Cytocompatibility studies were carried out according to the direct contact test of the ISO 10993−5:1999 standard for the simultaneous evaluation of the effect of the polymer network and the leached substances, such as unreacted monomers. Fibroblast showed an excellent viability (96−100%) when cultured on any hydrogel prepared (Figure 5), indicating that $ZnMA_2$, 1VI, and 4VI do not deteriorate the cytocompatibility of the pHEMA hydrogels and that no toxic substances are leaked from the networks.

ACT Loading and Release. Although both ACT and ETOX exhibit similar ability to inhibit human CA isoform II and are active at the nanomolar range,[52] relevant physicochemical differences between both molecules can be highlighted. CAIs bind in the active site of the enzyme in deprotonated state, coordinating to zinc, whereas the basic amino acids serve as proton acceptors. Therefore, the lower the pK_a, the more favorable the binding is. ACT is more acidic (pK_a 7.4) and significantly less lipophilic (Log P = −0.26) than ETOX (pK_a 8.0; Log P = 2.01).[53] Compared with ETOX, ACT is more ionized, and its solubility is greater at physiological pH 7.4. Although both CAIs obey Lipinski "rule of 5" properties and show good membrane permeability, ACT has seven hydrogen bond acceptors and three hydrogen bond donors, whereas ETOX has just five hydrogen bond acceptors and two hydrogen bond donors. Therefore, ACT may be anchored to the active site of the enzyme through more hydrogen bonds.[53] Drug loading experiments were designed to have the same number of molecules of ACT or ETOX in the volume of medium in which the hydrogels were immersed. Therefore, the first consequence of the physicochemical differences between ACT and ETOX was that the loading experiments with the latter had to be carried out by immersion of the hydrogels in an aqueous suspension because of the low solubility of ETOX. Loading with ACT was carried out by immersion in 0.2 g/L solution.

Table 3. ACT Loaded, Network/Water Partition Coefficients, ACT Released in NaCl 0.9% Solution, and Release Rate Constants Obtained after Fitting to the Square-Root Kinetics[a]

formulation	loading (mg/g)	$K_{N/W}$	ACT released at 48 h (mg/g)	K_H (% $h^{-0.5}$)	R^2
0	1.22 (0.10)	5.40 (0.18)	1.17 (0.04)	24.20 (2.05)	0.994
A	1.50 (0.30)	6.67 (1.46)	0.87 (0.04)	10.48 (0.53)	0.962
B	1.18 (0.36)	5.11 (1.77)	0.74 (0.06)	11.67 (0.26)	0.967
C	1.48 (0.20)	6.63 (0.96)	0.92 (0.13)	10.56 (0.47)	0.991
D	1.74 (0.12)	7.79 (0.58)	1.16 (0.02)	14.07 (2.98)	0.946
E	3.37 (0.03)	16.40 (0.16)	1.64 (0.05)	6.86 (0.18)	0.995
F	3.16 (0.25)	15.35 (1.26)	1.87 (0.20)	8.49 (0.45)	0.995
G	1.51 (0.10)	6.52 (0.48)	0.68 (0.04)	8.61 (0.71)	0.948
H	1.38 (0.10)	5.90 (0.50)	0.64 (0.04)	8.99 (0.79)	0.955
I	3.15 (0.29)	15.29 (1.47)	1.61 (0.18)	7.31 (0.04)	0.994
J	3.28 (0.15)	15.64 (0.72)	2.46 (0.30)	13.04 (0.16)	0.993

[a] Mean values and, in parentheses, standard deviations (n = 6).

Copolymerization of HEMA with $ZnMA_2$ solely or with HEAA did not significantly modify the amount of ACT uptaken by the hydrogels (Table 3). These hydrogels retained a small proportion of the zinc ions incorporated during synthesis, and thus no specific drug−network interactions could be established. A slight improvement in the loading was recorded for formulations having 1VI. In contrast, hydrogels bearing 4VI moieties showed a remarkably greater ability (two-fold) to load ACT (Table 3). The network/water partition coefficient, $K_{N/W}$, values obtained for formulations E, F, I, and J almost triplicate the values recorded for the other hydrogels. No further improvement was achieved by adding ACT as template during polymerization. This means that by using the functional monomers that mimic the best components of the CA receptor, it is feasible to endow the hydrogels with high affinity for ACT. Such a notable increase in affinity was also evidenced in a better control of drug release (Figure 6). Control hydrogels (formulation 0) rapidly released the ACT loaded. Copolymerization with functional monomers that resemble the functionalities of the components of the natural receptor at the active site significantly decreased the ACT release rate. Most hydrogels required 15 days to complete the release. Hydrogels A and B showed a certain decrease in ACT release rate compared with control hydrogels, which could be due to a slight increase in the mesh size of the network owing the divalent Zn ions connecting neighbor methacrylic acid mers. The release profiles fitted quite well to the square root kinetics, and the hydrogels E, F, and I showed the lowest release rate (Table 3). Imprinted hydrogels (i.e, formulations B, D, F, H, and J) seem to release ACT faster than the corresponding nonimprinted networks (Figure 6), although statistically significant differences were recorded only for formulation F compared with E and for formulation J compared with I (t test, $\alpha < 0.01$). The reasons behind this behavior are not clear but could be related to small changes in the microstructure of the hydrogels caused by the presence of ACT molecules during polymerization. The removal of the template molecules may have opened paths into the network for an easier entrance/exit of subsequent drug molecules. In fact, the synthesis in the presence of template molecules caused an increase in the degree of swelling of the imprinted networks compared with the nonimprinted ones (Table 2).

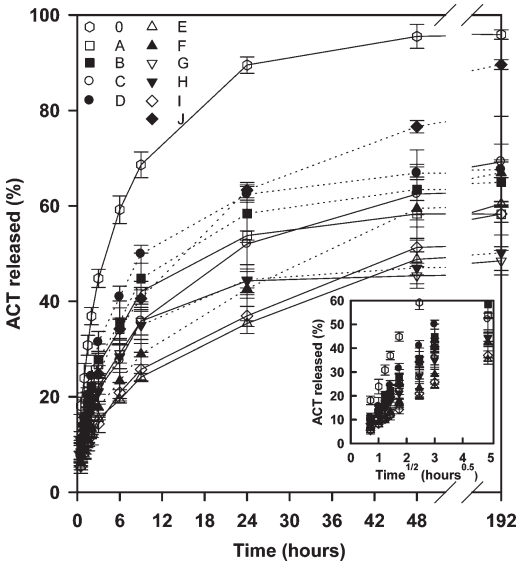

Figure 6. ACT release profiles in 0.9% NaCl medium from pHEMA hydrogels containing diverse functional comonomers. Continuous and dotted lines correspond to nonimprinted and ACT-imprinted networks, respectively. Codes as in Table 1. The insert shows data used for the fitting to the square-root kinetics.

ETOX Loading and Release. The loading of ETOX was carried out by immersion of the hydrogels in aqueous suspensions of the drug because of its limited solubility (21.38 mg/L). The suspensions contained the same number of molecules of ETOX per liter as in the case of ACT. The hydrogels loaded less ETOX than ACT, which may be due to the fact that the drug first has to dissolve to be available to interact with the network. Nevertheless, the hydrogels (even the control one) showed remarkably high affinity for ETOX (network/water partition coefficients above 36), which suggest unspecific hydrophobic adsorption to the pHEMA network. pHEMA-$ZnMA_2$ hydrogels containing 4VI were again those with greater ability to host ETOX and exhibited 90% greater $K_{N/W}$ values than the other hydrogels (Table 4), which indicates the contribution of specific interactions with the biomimetic pockets. The hydrogels sustained the release of ETOX for 2 weeks, after which the amount released was still <50% (Figure 7). The release rate decreased after 72 h, which could be due to the attainment of equilibrium between the free drug in the medium and the drug bound to the hydrogel due to the high drug-network affinity. It should be also noticed that the volume of the medium, although enough to dissolve the whole ETOX dose loaded by the hydrogels, was

Table 4. ETOX Loaded, Network/Water Partition Coefficient, ETOX Released in NaCl 0.9% Solution, And Release Rate Constants Obtained after Fitting to the Square-Root Kinetics[a]

formulation	loading (mg/g)	$K_{N/W}$	ETOX released at 48 h (mg/g)	K_H (% $h^{-0.5}$)	R^2
0	0.99 (0.17)	45.70 (7.82)	0.43 (0.06)	7.03 (0.66)	0.969
A	0.91 (0.12)	42.11 (5.64)	0.34 (0.04)	7.03 (0.46)	0.957
B	0.80 (0.16)	36.86 (7.55)	0.28 (0.04)	6.70 (0.48)	0.945
C	0.81 (0.14)	37.38 (6.40)	0.28 (0.05)	7.29 (0.97)	0.926
D	1.01 (0.04)	46.73 (1.92)	0.42 (0.02)	7.86 (0.27)	0.954
E	1.51 (0.07)	70.36 (3.45)	0.35 (0.03)	4.81 (0.18)	0.954
F	1.50 (0.18)	69.84 (8.27)	0.36 (0.03)	4.98 (0.45)	0.907
G	1.00 (0.02)	46.26 (1.08)	0.42 (0.03)	8.53 (0.22)	0.971
H	0.95 (0.11)	44.04 (5.18)	0.36 (0.01)	7.61 (0.99)	0.956
I	1.55 (0.12)	72.32 (5.44)	0.35 (0.03)	4.02 (0.63)	0.921
J	1.71 (0.18)	79.38 (7.33)	0.48 (0.06)	4.92 (0.44)	0.962

[a] Mean values and, in parentheses, standard deviations ($n = 6$).

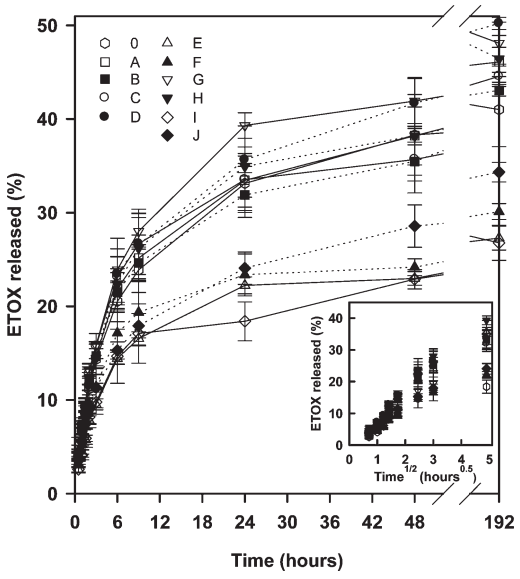

Figure 7. ETOX release profiles in 0.9% NaCl medium from pHEMA hydrogels containing diverse functional comonomers. Continuous and dotted lines correspond to nonimprinted and ACT-imprinted networks. Codes as in Table 1. The insert shows data used for the fitting to the square-root kinetics.

limited to 5 mL to resemble the small volume of lachrymal fluid that could be available on the cornea for the release of the drug from a medicated SCL. The release data obtained in the first 48 h were fitted to the square-root kinetics (Table 4). Hydrogels 0, A, and B behaved very similar probably because of the fact that unspecific hydrophobic interactions drive the binding of the drug to the network and small differences in mesh size are less relevant for drug diffusion than in the case of the water-soluble ACT. The most biomimetic hydrogels (formulations E, F, I, and J) sustained better the release highlighting the role of an adequate combination of functional groups in the ability of the hydrogels to host the drug with high affinity and to regulate its release rate. Differences in ETOX loading/release between ACT-imprinted and nonimprinted hydrogels were minor and did not follow a clear trend.

CONCLUSIONS

The knowledge of the physiological receptors with which drugs interact to exert the therapeutic effect has been used so far for the chemical optimization of the drugs or the search of new candidates with improved pharmacological efficacy and safety. Although still few, previous works have suggested that the structure of the physiological receptor can also be used as the model to follow in the design of optimized drug delivery systems.[23,34,35] We have here demonstrated that mimicking the active site of CA, networks with high affinity for inhibitor drugs (CAIs) can be created. Biomimetic networks can load more drug and control better drug release than conventionally synthesized pHEMA hydrogels, being useful for the development of advanced controlled release systems. Nevertheless, aspects such as optical transparency (for application as drug-eluting SCLs), the effect of thickness on drug release length, and long-term durability of the biomimetic receptors (from both the point of view of time between preparation and use and of any application that involves loading/release cycles) require further studies to elucidate fully the practical potential of enzyme-mimicking networks.

AUTHOR INFORMATION

Corresponding Author

*Fax: 34-981547148. E-mail: carmen.alvarez.lorenzo@usc.es.

ACKNOWLEDGMENT

Work supported by MICINN (SAF2008-01679) and FEDER (Spain) and Fundação para Ciência e Tecnologia (FCT, Praxis grant SFRH/BD/40947/2007, Portugal). We thank C. Fernández Masaguer and J. González Parga for their help with the synthesis of 4VI and A. Rey-Rico for help with the cytocompatibility tests.

REFERENCES

(1) Fechtner, R. D.; Godfrey, D. G.; Budenz, D.; Stewart, J. A.; Stewart, W. C.; Jasek, M. C. *Cornea* **2010**, *29*, 618–621.
(2) Bock, R.; Meier, J.; Nyul, L. G.; Hornegger, J.; Michelson, G. *Med. Image Anal.* **2010**, *14*, 471–481.
(3) Grieshaber, M. C.; Pienaar, A.; Olivier, J.; Stegmann, R. *Invest. Ophthalmol. Visual Sci.* **2009**, *51*, 1498–1504.
(4) Tsai, J. C.; Kanner, E. M. *Expert Opin. Emerging Drugs* **2005**, *10*, 109–118.
(5) Urtti, A. *Adv. Drug Delivery Rev.* **2006**, *58*, 1131–1135.
(6) Leino, M.; Urtti, A. Recent Developments in Anti-Glaucoma Drug Research. In *Ocular Therapeutics and Drug Delivery*; Reddy, I. K., Ed.; Technomic Publishing Co., Inc.: Lancaster PA, 1996, pp 245−257.
(7) Wajs, G.; Meslard, J. C. *Crit. Rev. Ther. Drug Carrier Syst.* **1986**, *2*, 275–289.
(8) Alvarez-Lorenzo, C.; Hiratani, H.; Concheiro, A. *Am. J. Drug Delivery* **2006**, *4*, 131–151.
(9) Xinming, L.; Yingde, C.; Lloyd, A. W.; Mikhalovsky, S. V.; Sandeman, S. R.; Howel, C. A.; Liewen, L. *Contact Lens Anterior Eye* **2008**, *31*, 57–64.
(10) Alvarez-Lorenzo, C.; Yañez, F.; Concheiro, A. *J. Drug Delivery Sci. Technol.* **2010**, *20*, 237–248.
(11) White, C. J.; Byrne, M. E. *Expert Opin. Drug Delivery* **2010**, *7*, 765–780.
(12) Karlgard, C. C.; Wong, N. S.; Jones, L. W.; Moresoli, C. *Int. J. Pharm.* **2003**, *257*, 141–151.
(13) Boone, A.; Hui, A.; Jones, L. *Eye Contact Lens* **2009**, *35*, 260–267.
(14) Anne, D.; Heïdi, B.; Yves, M.; Patrick, V. *J. Biomed. Mater. Res.* **2007**, *82A*, 41–51.
(15) Gulsen, D.; Chauhan, A. *Int. J. Pharm.* **2005**, *292*, 95–117.
(16) Gulsen, D.; Li, C. C.; Chauhan, A. *Curr. Eye Res.* **2005**, *30*, 1071–1080.
(17) Kapoor, Y.; Chauhan, A. *Int. J. Pharm.* **2008**, *361*, 222–229.
(18) Miranda, M. N.; Garcia-Castineiras, S. *CLAO J.* **1983**, *9*, 43–48.
(19) Takao, S.; Rei, U.; Haruyasu, T.; Kenji, U.; Akira, M. *J. Appl. Polym. Sci.* **2005**, *98*, 731–735.
(20) dos Santos, J. F.; Couceiro, R.; Concheiro, A.; Torres-Labandeira, J. J.; Alvarez-Lorenzo, C. *Acta Biomater.* **2008**, *4*, 745–755.
(21) Alvarez-Lorenzo, C.; Concheiro, A. *J. Chromatogr., B* **2004**, *804*, 231–245.
(22) Hiratani, H.; Alvarez-Lorenzo, C. *Biomaterials* **2004**, *25*, 1105–1113.
(23) Venkatesh, S.; Sizemore, S. P.; Byrne, M. E. *Biomaterials* **2007**, *28*, 717–724.
(24) Ali, M.; Horikawa, S.; Venkatesh, S.; Saha, J.; Hong, J. W.; Byrne, M. E. *J. Controlled Release* **2007**, *124*, 154–162.
(25) Alvarez-Lorenzo, C.; Yanez, F.; Barreiro-Iglesias, R.; Concheiro, A. *J. Controlled Release* **2006**, *113*, 236–244.
(26) Bergmann, N. M.; Peppas, N. A. *Prog. Polym. Sci.* **2008**, *33*, 271–288.
(27) Kryscio, D. R.; Peppas, N. A. *AIChE J.* **2009**, *55*, 1311–1324.
(28) Hiratani, H.; Mizutani, Y.; Alvarez-Lorenzo, C. *Macromol. Biosci.* **2005**, *5*, 728–733.

(29) Ito, K.; Chuang, J.; Alvarez-Lorenzo, C.; Watanabe, T.; Ando, N.; Grosberg, A. Yu. *Prog. Polym. Sci.* **2003**, *28*, 1489–1515.
(30) Hiratani, H.; Fujiwara, A.; Tamiya, Y.; Mizutani, Y.; Alvarez-Lorenzo, C. *Biomaterials* **2005**, *26*, 1293–1298.
(31) Yanez, F.; Chianella, I.; Piletsky, S. A.; Concheiro, A.; Alvarez-Lorenzo, C. *Anal. Chim. Acta* **2010**, *659*, 178–185.
(32) Chianella, I.; Karim, K.; Piletska, E. V.; Preston, C.; Piletsky, S. A. *Anal. Chim. Acta* **2006**, *559*, 73–78.
(33) Hilt, J. Z.; Byrne, M. E. *Adv. Drug. Delivery Rev.* **2004**, *56*, 1599–1620.
(34) Venkatesh, S.; Saha, J.; Pass, S.; Byrne, M. E. *Eur. J. Pharm. Biopharm.* **2008**, *69*, 852–860.
(35) Ali, M.; Byrne, M. E. *Pharm. Res.* **2009**, *26*, 714–726.
(36) Abbate, F.; Casini, A.; Scozzafava, A.; Supuran, C. T. *Bioorg. Med. Chem.* **2004**, *14*, 2357–2361.
(37) Lindskog, S. *Pharmacol. Ther.* **1997**, *74*, 1–20.
(38) Di Fiore, A.; Pedone, C.; Antel, J.; Waldeck, H.; Witte, A.; Wurl, M.; Scozzafava, A.; Supuran, C. T.; De Simone, G. *Bioorg. Med. Chem. Lett.* **2008**, *18*, 2669–2674.
(39) Overberger, C. G.; Vorchheimer, N. *J. Am. Chem. Soc.* **1963**, *85*, 951–955.
(40) Janina, A.; Meir, W. *J. Heterocycl. Chem.* **1988**, *25*, 915–916.
(41) Alvarez-Lorenzo, C.; Hiratani, H.; Gomez-Amoza, J. L.; Martinez-Pacheco, R.; Souto, C.; Concheiro, A. *J. Pharm. Sci.* **2002**, *91*, 2182–2192.
(42) Sabel, C. E.; Neureuther, J. M.; Siemann, S. *Anal. Biochem.* **2010**, *397*, 218–226.
(43) Kim, S. W.; Bae, Y. H.; Okano, T. *Pharm. Res.* **1992**, *9*, 283–290.
(44) Korsmeyer, R. W.; Gurny, R.; Doelker, E.; Buri, P.; Peppas, N. A. *Int. J. Pharm.* **1983**, *15*, 25–35.
(45) Nicolson, P. C.; Vogt, J. *Biomaterials* **2001**, *22*, 3273–3283.
(46) Jithunsa, M.; Tashiro, K.; Nunes, S. P.; Chirachanchai, S. *Polym. Degrad. Stab.* **2008**, *93*, 1389–1395.
(47) Morcellet, M. *Polym. Bull.* **1984**, *12*, 127–132.
(48) Liu, K. J.; Gregor, H. P. *J. Phys. Chem.* **1965**, *69*, 1252–1259.
(49) Pekel, N.; Sahiner, N.; Güven, O.; Rzaev, Z. M. O. *Eur. Polym. J.* **2001**, *37*, 2443–2451.
(50) Holden, B. A.; Mertz, G. W. *Invest. Ophthalmol. Visual Sci.* **1984**, *25*, 1161–1167.
(51) Bruce, A. *Contact Lens Anterior Eye* **2003**, *26*, 189–196.
(52) Supuran, C. T.; Scozzafava, A. *Bioorg. Med. Chem.* **2007**, *15*, 4336–4350.
(53) Remko, M.; von der Lieth, C. W. *Bioorg. Med. Chem.* **2004**, *12*, 5395–5403.